How to overcome the demagnetization of superconducting Halbach arrays?

M Houbart[1], J-F Fagnard[1], J Dular[2], A R Dennis[3], D K Namburi[4], J H Durrell[3], C Geuzaine[1], B Vanderheyden[1] and P Vanderbemden[1]

[1] University of Liege, Department of Electrical Engineering and Computer Science, B-4000 Liege, Belgium
[2] TE-MPE-PE, CERN, Geneva, Switzerland
[3] University of Cambridge, Bulk Superconductivity Group, Cambridge CB2 1PZ, United Kingdom
[4] Quantum Sensors Group, James Watt School of Engineering, University of Glasgow, Glasgow G12 8QQ, United Kingdom

E-mail: `michel.houbart@uliege.be`

Abstract. Assembling trapped-field superconducting magnets with mutually orthogonal magnetizations directions in a Halbach array configuration offers the prospect of generating both high fields and large field gradients. A major issue when assembling bulk superconductors in a Halbach array, however, consists in the alteration of the initial current density distribution during the assembly process. This reorganization of supercurrent loops limits the field generated by the system.

We investigate two methods for reducing this demagnetization effect. The first method consists of using stacked tapes instead of bulk superconductors. For the second method, we propose a procedure leading to a re-magnetizing the superconductors of the array after the assembly. The procedure consists in putting two superconductors on top of one another, magnetizing them along the vertical direction, and then keeping the pair in place while two other superconductors, magnetized in an horizontal direction, are approached from left and right. The top central sample is then removed from the array, thereby providing the desired re-magnetization of the bottom one. The benefits of this procedure was investigated by finite element modelling and experiments carried out at 77 K both with bulk $YBa_2Cu_3O_{7-x}$ superconductors ($\sim$14×14×14 mm^3) and with stacks of 2G $YBa_2Cu_3O_{7-x}$ tapes from Superpower ($\sim$12×12×12 mm^3).

The flux density measured above the array is compared to analytical results and finite element simulations. The results show that a re-magnetization of the central sample occurs, which allows the maximum field generated with Halbach arrays made of 3 bulk superconductors or three stacked tapes to be increased by 5% and 11% respectively. Numerical modelling shows that using a taller top sample with this method allows to recover almost the full potential of the array.

Bulk superconductor, stacked tapes, trapped-field magnet, magnetic field gradient, interacting bulk superconductors, flux pinning

1. Introduction

An efficient method to generate a significant magnetic flux density gradient compactly is to combine several permanent magnets in a Halbach array. In the most common Halbach array configuration [1], the magnetizations of the neighbouring magnets are perpendicular to each other. This specific configuration causes a concentration of the magnetic flux density on a single side of the arrangement. Although it has been demonstrated that substantial magnetic field strengths and gradients can be attained with this technique [2–5], the use of conventional permanent magnets in its implementation still imposes the fundamental limitation of the saturation magnetization ($\mu_0 M_{\rm sat} \sim 1.4$ T for Nd-Fe-B [6, 7] and 2.4 T for soft ferromagnetic Fe-Co alloys [6]).

In order to overcome this limitation, we have proposed assembling a Halbach array from superconducting trapped-field magnets [8]. Such trapped-field magnets consist of centimetric-size bulk superconductors in which persistent current loops are induced and trapped permanently. Since they do not suffer from any saturation magnetization [9–12], superconducting magnets are attractive candidates for replacing permanent magnets in Halbach arrays. Hull *et al* investigated theoretically this idea for a circular Halbach array [13] and in our work we investigated experimentally and numerically a linear Halbach array made of bulk superconductors [8]. Unlike permanent magnets, however, bulk superconducting trapped-field magnets are prone to partial demagnetization when they are subjected to a time-varying magnetic field component perpendicular to their permanent magnetization. We showed numerically that when 3 magnetized $YBa_2Cu_3O_{7-x}$ bulk superconductors are assembled in a Halbach array, the superconductors located at the sides of the array produce persistent current loops in the central superconductor, as illustrated schematically in Figure 1. These current loops are induced during the assembly process mainly in the vicinity of the lateral side of the central superconductor. The current density in these regions was found to flow in loops perpendicular to the direction of the magnetization of the peripheral samples (x-axis in Figure 1); these current loops oppose the field generated by the closest neighbouring sample. Similar current reorganization has been reported in "crossed-field" experiments [14–21]. In these studies, a magnetized superconductor is subjected to a time-varying external magnetic field perpendicular to its main axis of magnetization, which is analogous to the conditions encountered when assembling a linear superconducting Halbach array. For a Halbach array made of superconducting trapped-field magnets, we showed experimentally [8] that this partial demagnetization results in a reduction of 13% of the maximum magnetic flux density generated by the Halbach assembly and thus limits its performance.

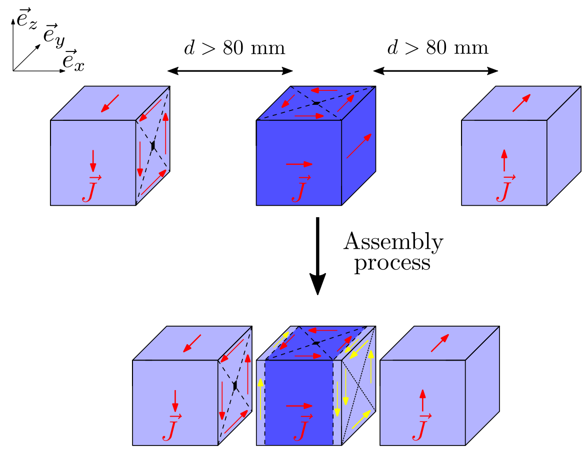

Figure 1. Schematic representation of the modification of the current density occurring during the assembly process of a superconducting Halbach array made of 3 magnetized $YBa_2Cu_3O_{7-x}$ bulk superconductors. The red arrows shows the current distribution in the samples before assembling the array whereas the yellow arrows shows the modifications induced by the interaction during the assembly process.

Two methods are explored in this work to overcome the alteration of superconducting currents arising during the assembly process of superconducting Halbach arrays. The first method consists in replacing each bulk superconductors by a stack of coated conductor tapes. Such "quasi-bulks" made of stacked tapes exhibit trapped-field performance comparable to bulk superconductors [12, 22, 23] and are less affected by crossed-field demagnetization [15, 24–27]. Similarly to bulk superconductors, these stacked tapes samples are not constrained by any saturation magnetization. Thanks to that, the field generated by a Halbach array made of superconducting stacked tapes is expected to exhibit improvement through the reduction of operating temperature or the use of larger sample. Unlike bulk superconductors, however, the induced supercurrents in stacked tapes cannot flow along a direction perpendicular to the stack. As a result, the loops resulting from the approach of the two side superconductors, as shown in yellow in Figure 1, cannot be generated. In the second method, an additional superconductor placed above the central one is used. This additional superconductor is magnetized simultaneously with the central one and removed after the assembly process. The removal of the additional superconductor generates a time-varying field applied on the central superconductor in order to re-magnetize it. This method, described in more details in the following sections, will be shown to be an efficient way to overcome the demagnetization of superconducting Halbach array so that they could provide their full potential.

2. Experimental methods

In this work, two sets of experiments are carried out with the experimental rig presented in our earlier work [8]. This experimental rig enables three magnetized superconductors to be moved in reproducible way and to be assembled as a linear Halbach array at 77 K. To do so, the samples are initially magnetized sequentially at 77 K using a field cooling process starting from 1.2 T and gradually removing the magnetic field at a rate of 1 mT s^{-1}. After that, the arrangement is assembled by translating the outer samples towards the central one at 0.6 mm s^{-1}. A 45 minute delay is allowed for magnetic relaxation both after the magnetization process and after the approach.

After assembly, the magnetic flux density produced by the resulting array is measured at a distance of 1 mm above the upper surface of the central superconductor. The profile of the magnetic flux density component perpendicular to the array (B_z) is then examined to assess the performance of each array considered. This analysis is conducted along the alignment direction of the configuration, referred to as line x. A schematic picture of the position of this line relative to the assembled Halbach array is presented in Figure 2.

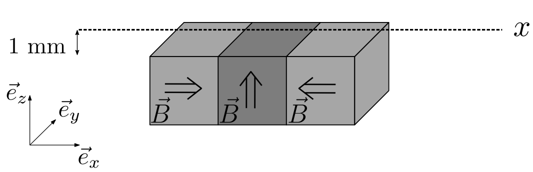

Figure 2. Schematic representation of the Hall probe mapping performed on the assembled array in each experiment.

2.1. *Superconducting Halbach array made of 3 stacked-tape samples*

The goal of the first set of experiments is to prevent the superconducting currents induced in the central sample during the assembly from forming loops perpendicular to its main axis of magnetization. As shown schematically in Figure 3, when the central sample consists of several superconducting tapes stacked along the z direction, it is impossible for current loops to form in the y-z plane to form the assembly.

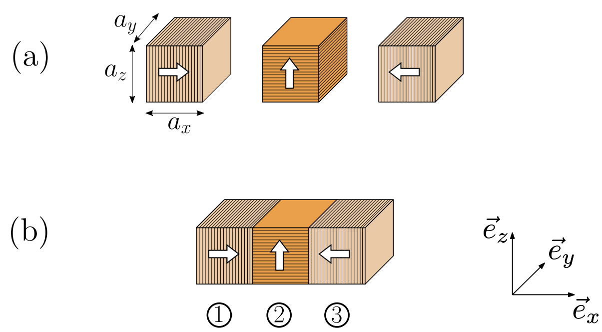

Figure 3. Schematic representation of a superconducting Halbach array made of 3 magnetized stacked tapes before (a) and after (b) the assembly process.

The samples used in this experiment are made of stacks of 120 second generation (2G) $YBa_2Cu_3O_{7-x}$ tapes from Superpower, with copper stabilizer. Each tape within the stacks originated from a single HTS tape of 12 mm in width, 0.1 mm in thickness. The critical current at 77 K in self-field I_c if is the range of ~240 A. The insulation between the superconducting layers is ensured by the different buffer layers and the substrate within the tape, no additional insulation is added between individual tapes. The samples obtained measure 12.6 mm in height and have a square section parallel to the ribbon with a side of 12.1 mm. The trapped field at 77 K, measured 1 mm above the centre of the stack, after a field cooled process starting from 1.2 T, is equal to 200 mT ±2 mT.

2.2. *Alternative assembly of superconducting Halbach array*

An alternative assembly process of the Halbach array is proposed and investigated in the second set of experiments described in this work. The idea of the method is to apply a time-varying field mainly directed along the z-direction on the central sample after the assembly process. Provided that the applied field amplitude is sufficient, a re-organization of the supercurrents flowing in the central sample is expected and the central sample will be re-magnetized at least partially. In order to achieve this, the proposed method makes use of the trapped field of an additional magnetized superconductor as a source of re-magnetizing field. The procedure is described step by step below and illustrated in Figure 4.

a) The magnetization process of the peripheral samples remains unchanged. The central sample, however, is magnetized simultaneously with an additional superconductor placed just above it. The additional sample and the central sample are maintained in contact and their c-axes are kept aligned during the whole magnetization process, as shown in Figure 5.

b) The central and the additional samples are maintained stationary while the peripheral superconductors are approached from left and right.

c) The additional sample is removed from the array. The force required to extract the additional sample is numerically evaluated not to exceed 15 N for the samples used in this work. This allows this second step to be performed manually by the experimenter. The retracting motion is expected to decrease progressively the z-component of the magnetic flux density experienced by the central superconductor and thus to induce the desired re-magnetization.

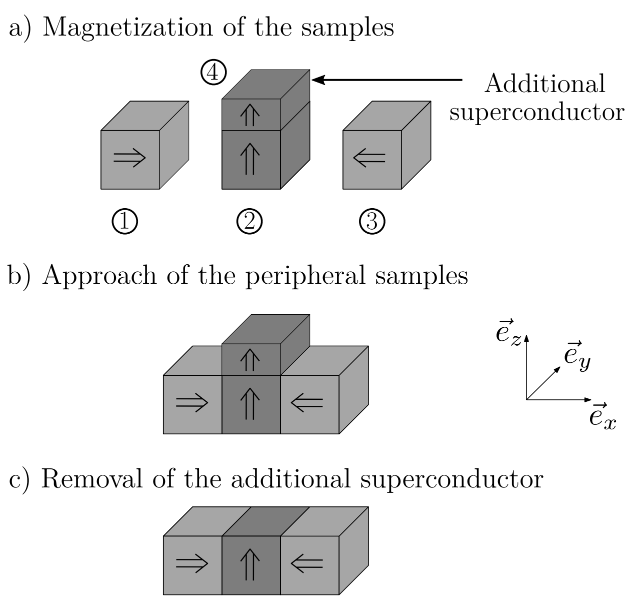

Figure 4. Schematic representation of the alternative method proposed for assembling a superconducting Halbach array. The samples ① and ③ are the peripheral samples, sample ② is the central sample, and sample ④ is the additional superconductor used in the alternative assembly process.

This method was investigated experimentally both with bulk superconducting $YBa_2Cu_3O_{7-x}$ samples manufactured by the TSMG method [28–31] and with stacks of 120 2G $YBa_2Cu_3O_{7-x}$ tapes from Superpower described in the section above. Photographs of the central and the additional samples, as well as their relative positions during the magnetizing process (step a)) are shown in Figure 5. It should be noted that the peripheral samples are not yet visible in Figure 5, since they are magnetized separately.

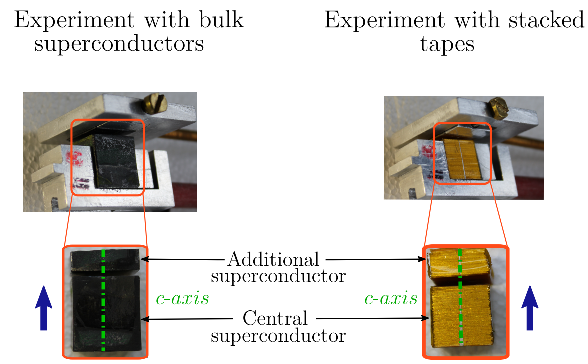

Figure 5. Photograph of the central and additional samples during the magnetization process. The blue arrows represent schematically the main direction of the trapped flux density in both the central and additional superconductors after the magnetization process.

Importantly, the time-varying field experienced by the peripheral samples during the re-magnetization step should be limited as much as possible in order to avoid partially demagnetizing them. The dimensions along x and y of the additional sample are therefore made as close as possible to those of the central superconductor. The height of the additional sample (along z) has to be large enough so that its trapped field is sufficient to re-magnetize the central superconductor. The dimensions and the trapped field at 77 K of the bulk superconductors are presented in Table 1.

Table 1. Dimensions and trapped field at 77 K of the bulk superconductors involved in the superconducting Halbach array. Sample 4 correspond to the additional bulk superconductor.

Sample number	a_x [mm]	a_y [mm]	a_z [mm]	Trapped field [mT]
①	15.2	14.1	14.1	440
②	14.4	14.4	15.9	466
③	14.3	14.3	14.5	461
④	14.2	14.3	4.8	430

As can be noticed in Table 1, the height of the additional bulk sample is approximately one third of those of the cuboid samples used in the array, while its trapped field is $\sim 5 - 6\%$ smaller. When the experiment is carried out with stacked tapes in place of bulk superconductors, the samples ① to ③ in Figure 4 corresponds to the stacked tapes of the first experiment, thus presenting an individual trapped field 1 mm above their top surface equal to 200 mT ±2 mT. Regarding the additional stacked tape sample, i.e. sample ④ in Figure 4, the squared cross-section parallel to the tape planes is 12.1×12.1 mm^2 and the height is 5.3 mm. The trapped field measured 1 mm away from the top surface of the sample ④ at 77 K is 173 mT. Since the central and the additional samples have to be magnetized simultaneously, the total height of the "central + additional" samples stacked together should not exceed the air gap of the electromagnet used for magnetizing them. The electromagnet used in this work has an air gap of approximately 22 mm, which explains why experiments could not be carried out with taller superconductors.

3. Models

3.1. Analytical model

In this work, we use an analytical model based on Biot-Savart law, as formulated in [8], to compute the distribution of the magnetic flux density $\vec{B}$ generated by a fully magnetized cubic bulk superconductor. This model essentially assumes that the superconductor is in the critical state (Bean model [32]) and that the sample exhibits a critical current density J_c that is independent of the applied magnetic field.

The same model is also applied to compute the magnetic flux density generated by a magnetized superconducting stack of tapes. In this case, the model considers a homogeneous material characterized by a constant and field-independent engineering critical current density J_e and ignores the layered structure of the stack.

For each sample, the current density value used in the model is adjusted to reproduce the individual trapped field measured after the magnetic relaxation and presented in the previous section. This procedure leads to $J_c = 2\times10^8$ Am^{-2} and $J_e = 1.3\times10^8$ Am^{-2} for bulks and for stacked tapes respectively. It should be noted that the rather modest value of J_e for the stacked tapes sample here is consistent with the fact that the tapes used have a current I_c of the order of ∼240 A, measured in self-field. Considering an $I_c(B)$ dependence one might indeed expect the engineering current of the fully magnetized stack to be smaller than the value deduced from individual tape samples [33–35]. It should be also emphasized that the J_c and J_e values mentioned above refer to the amplitude of currents after a waiting time of ∼45 minutes after the magnetization process, resulting in a further decrease of the current density. Using tapes with e.g. 500 A nominal current at 77 K and self-field would result in an engineering current density J_e comparable to the J_c of the bulk, large grain sample.

When several superconductors are assembled in a linear Halbach array, the model assumes that the supercurrent loops in each superconductor are not affected by any relative motion between them, i.e. that no demagnetization of the samples occurs during the assembly process. The total magnetic flux density at any point of space is calculated as the sum of the magnetic flux densities generated by each superconductor. This analytical model is therefore used to estimate the flux density generated by the array in an ideal case, i.e. without demagnetization.

3.2. Finite element model

A numerical tool was developed in *GetDP* within the Life-HTS toolkit in order to obtain a qualitative understanding of the current distribution alteration occurring during the assembly of the array. The finite element model is based on the mixed h-ϕ-a formulation in 3D developed in [36]:

- The behaviour of superconducting regions is described with a h-formulation as recommended in [36]. The meshing of these regions is forced to remain identical despite the motion, so that no projection error is introduced when computing the time-derivative from one mesh to another.
- An a-formulation is used for describing the non-conducting regions. The time-derivative involved in this formulation arising only in conducting regions, the mesh of the non-conducting regions is allowed to change from time step to time step without the need of any projection algorithm.
- Both formulations are coupled thanks to surface coupling terms computed at the common boundary between conducting and non-conducting regions. By construction, the mesh of these boundaries is also kept the same during the whole simulation. As a result, no projection error is introduced either.

The modelling of the motion is handled through the update of the position of the superconducting regions at each time step. Additionally, the a-field and the h-field calculated in the preceding time step are shifted appropriately to evaluate the time-derivatives [37]. The superconductors are meshed with hexahedron elements whose dimensions are approximately equal to 1/12 of the cube side, i.e. ∼ 1 mm.

3.2.1. Magnetization of bulk superconductors The magnetization of one bulk is simulated to compute the initial a-field and h-field distributions in the domain. A zero-field cooled process is simulated with a maximum applied field of 2.4 T, i.e. twice as high as the field actually experienced by the sample during the experimental field-cooled procedure. The successive increase and decrease of the field during this process is performed at a constant rate of 1 mT s^{-1}. For simplicity, the modelled bulk superconductor is assumed to be a perfect cube of dimensions 14×14×14 mm^3. The critical exponent is assigned a value of $n = 20$, a common value for $YBa_2Cu_3O_{7-x}$ bulk superconductors operating at 77 K [38]. The critical current density is assumed to be homogeneous and isotropic. For each individual bulk superconductor, the critical current density is set to 2.3×10^8 A m^{-2}. This choice ensures that, after the magnetic relaxation period of 45 minutes, the remaining current density circulating within the superconductor closely approximates the value deduced experimentally. The field distribution of the initial state (i.e. prior to any motion) is evaluated after a 45-minute period following the magnetization process.

The simultaneous magnetization of two superconductors is also modelled by applying the magnetizing field described above to two aligned cuboid bulk superconductors separated by a distance of 1.5 mm. This specific spacing value is chosen to ensure that the modelled samples are always separated by a distance greater than the mesh size imposed inside the superconductors. The additional superconductor is a cuboid of dimensions 14×14×h mm^3, where h is a parameter varying from 3 to 14 mm, so that the influence of the height of this additional superconductor on the re-magnetization of the central superconductor can be investigated.

3.2.2. Magnetization of stacked tapes For modelling the behaviour of stacked tapes, the same zero-field cooled process was applied to a superconducting cube of dimensions 12×12×12 mm^3. The critical exponent is still fixed to $n = 20$, the engineering critical current density is still assumed to be homogeneous and field-independent: its value is set to 1.7×10^8 A m^{-2} to match experimental trapped-field measurements. Furthermore, an anisotropic behaviour of the superconducting regions is considered in the simulation by introducing a linear resistive term in the power law used.

$$\vec{E} = \left[\frac{E_c}{J_e}\left(\frac{||\vec{J}||}{J_e}\right)^{n-1}\mathbb{1} + \mathrm{diag}(\rho_1, \rho_2, \rho_3)\right]\vec{J}, \qquad (1)$$

where ρ_i is equal to 10^{-8} Ω m in the direction perpendicular to the tapes, and to 0 in the other directions.

The simultaneous magnetization of two cubic stacked tapes separated by a distance of 1.5 mm is also simulated, ensuring a spacing between the modelled samples greater than the mesh size imposed inside the superconductors. The additional superconductor is a cuboid of dimensions 12×12×h mm^3, where h is a parameter varying from 3 to 12 mm.

3.2.3. Assembly of the array The modelling of the classic assembly of three identical cubic superconductors is carried out by considering an initial distance of 40 mm between neighbour samples. Such a distance is sufficient to consider negligible interactions between the superconductors [39] and the individually computed a-field and h-field distributions are therefore used as initial conditions. The separation distance is then gradually reduced at a rate of 1 mm s^{-1} until it reaches a final value of 0.5 mm.

The alternative assembly proposed in section 2.2 is simulated in two steps. In a first simulation, the distance between the central and the additional sample is set to 1.5 mm and the approach of the peripheral samples is modelled as described above. The a-field and h-field distributions at the final time step of the approach of the peripheral samples are then used as initial conditions for the second simulation. In the latter, the distance between the central and the additional superconductor samples is increased at a rate of 1 mm s^{-1} until it reaches a value of 40 mm.

4. Results and discussion

The numerical and experimental results are presented in the two following sections. We first consider the Halbach array containing superconducting stacked tapes instead of bulk superconductors. Second, we examine the effectiveness of the alternative assembly process described above.

4.1. Superconducting Halbach array made of 3 stacked tapes

The distributions of the current density in each stacked tape sample predicted by the finite element model, before and after the assembly are examined in Figure 6. For conciseness, the comparison is only examined in two cut planes. The first one (shown in blue in Figure 6) is the Oxz plane, where the origin O corresponds to the centre of the central superconductor. The second (shown in green in Figure 6) is parallel to $\vec{e}_y$ and $\vec{e}_z$ and cuts the central superconductor at 0.1 mm from its edge.

Before the assembly process, the supercurrents J_y crossing the Oxz plane (Plane 1 in Figure 6) are almost uniform with positive and negative signs for each half of the cross-section, as can be expected for three fully magnetized superconductors. The magnitude of the current density ($\sim 1.3\times10^8 \mathrm{Am}^{-2}$) is lower than the J_e of the stacked tape samples ($\sim 1.7\times10^8$ Am^{-2}) because of the flux creep occurring during the 45 min delay between the end of the magnetization and the

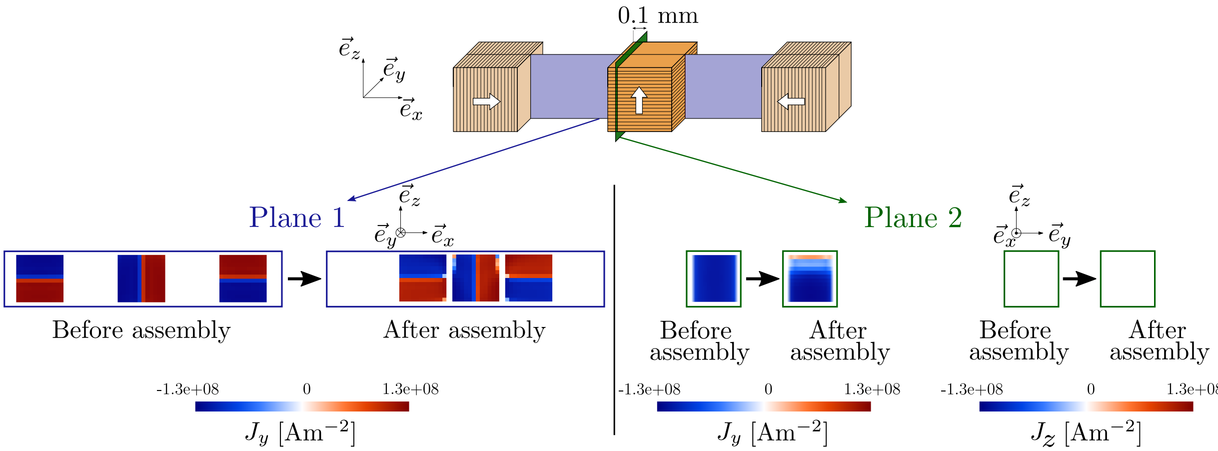

Figure 6. Comparison of the distribution of the y and z-components of the current density before and after the assembly of the Halbach array made of stacked tapes, as computed by the finite element model. The white arrows represent schematically the main direction of the trapped flux density in each sample. A field-independent critical current density of 1.7×10^8 A m^{-2} is considered in this simulation.

beginning of the assembly. Similarly, the supercurrents along the left face of the central superconductor (Plane 2 in Figure 6) are uniform as can be expected for square supercurrent loops. After the assembly, the current distribution is found to be altered, despite the strong anisotropy of the stacked tapes. As can be noticed in Figure 6, a current density re-organization occurs in the central stack during the assembly. Figure 7 illustrates a comparative representation of the current loops induced in either bulk superconductors or in stacked superconducting tapes. It can be observed in Figure 7 (b) that two features only appear with stacked tapes:

- Due to the layered structure, the supercurrents in the central sample continue to flow in loops perpendicular to the z-axis even after the assembly process. Although the main magnetization direction of the peripheral samples is parallel to $\vec{e}_x$, the magnetic flux density they produce on the lateral surface of the central sample exhibits a non-zero z-component, as shown with further details in appendix 1. The current reorganization observed in the central sample (illustrated by the yellow arrows in Figure 7 (b)) is thus most likely induced by this particular field component of the peripheral stacks, which increases as the peripheral samples are brought closer.
- The current density is mostly altered in a region close to the top face of the central sample. This result makes sense given that this region corresponds to the location where the z-component of the trapped field of the peripheral samples is positive and is the highest, as it may be observed in Figure 12 in appendix 1.

The alteration of the current distribution shown

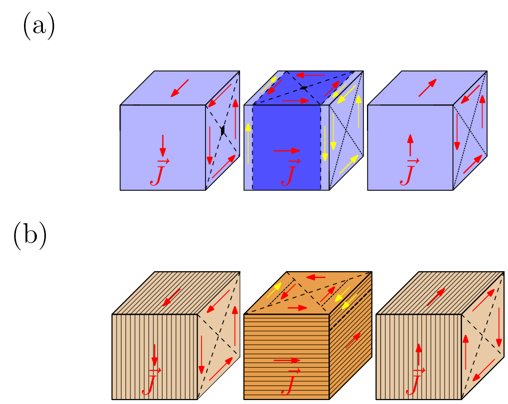

Figure 7. Comparison of the schematic modification of the current density after the assembly process for (a) bulk samples and (b) stacked tapes, as deduced from the finite element modelling results shown in Figure 6.

in Figure 7 (b) results in a reduction of the maximum magnetic flux density. To verify this statement, the finite element model is compared to the measurement results and to the predictions of the analytical model assuming that the current distribution remains unchanged during the assembly process. The results are summarized in Figure 8.

We first examine the flux density in the region above the peripheral samples of the array, i.e. $x <$ -6 mm or $x >$ 6 mm. In this region, both models are found to give very similar results that are also in agreement with experimental data. The coincidence of the finite element model and the analytical model assuming no demagnetization in this region is expected given that no significant current redistribution of the peripheral samples is predicted by the finite element

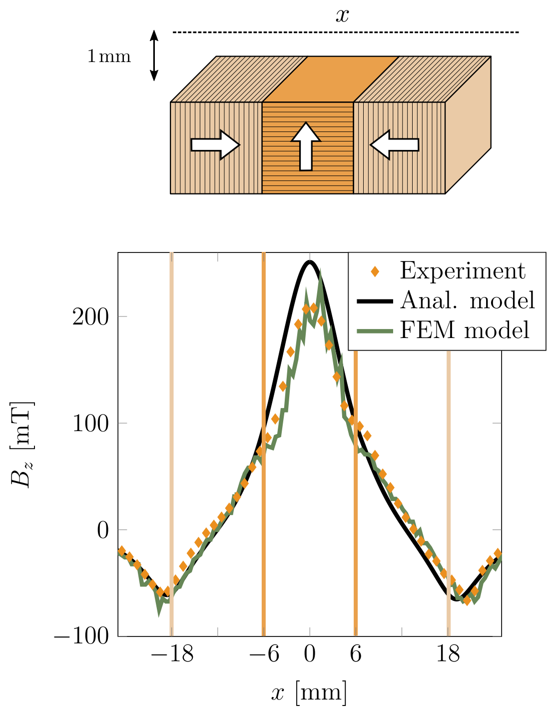

Figure 8. Evolution of the z-component of the magnetic flux density generated 1 mm away from the surface of a Halbach array made up of three superconducting stacked-tape samples along the line x. The orange vertical lines are located at the border of the superconducting samples. The experimental data are compared both to the finite element model and to an analytical model assuming a simple vector summation of the flux densities generated by each superconductors in the array and no alteration of the individual magnetization. The white arrows represent schematically the main direction of the trapped flux density in each sample.

model (see Figure 6). Now, focusing on the region above the central superconductor (-6 mm < x < 6 mm), a good agreement between finite element predictions and experimental data remains satisfying whereas the analytical model ignoring the current re-distribution significantly overestimates the field generated. This observation strongly suggests that a current alteration indeed occurs in the central sample and is correctly captured by the numerical simulations.

It can also be seen in Figure 8 that the maximum field measured experimentally is 205 mT , against the ideal value of ∼250 mT that would be obtained by the analytical model assuming no demagnetization. Given that the magnetic flux density measured above the central sample before assembly is 200 mT, the contribution of the peripheral samples over the centre of the array is thus almost completely erased by the supercurrent alteration occurring during the assembly. The practical conclusion to be drawn is that, although the layered structure of the stacked tapes leads to a current distribution that differs from that in bulk superconductors (see Figure 7), the deleterious impact on the resulting magnetic flux distribution above the array is found to be similar in both cases.

4.2. Alternative assembly of superconducting Halbach array

We investigate now the method proposed to re-magnetize the central sample after the assembly process. The efficiency of the proposed re-magnetization process as a function of the height of the additional superconductor is first investigated numerically. The y and z-components of the current density computed for bulk superconductors after the removal of the additional sample as well as the central field computed 1 mm away from the array are presented in Figure 9.

We first focus on the current density distribution in the green plane in Figure 9 (a) when no additional sample is considered (h = 0 mm). The distribution computed in this cut plane after the assembly differs significantly from the initial one, the situation is actually exactly the same as that depicted schematically in Figure 1. Then, examining only the y-component of the current density, it appears that the final supercurrent distribution varies when an additional sample is employed during the assembly procedure. More particularly, it can be observed that as the height of the additional sample increases, the final current distribution approaches the initial one. Besides, it can also be noticed that whatever the height of the additional sample, the final current distribution exhibits a non-zero z-component that was not present before the assembly process. In Figure 9 (b), the quantity $B_{\mathrm{c,ND}}$ denotes the field amplitude 1 mm above the centre (C) of the top surface of the central superconductor computed with the analytical model. Since the analytical model does not consider the demagnetization of the central sample induced by the peripheral samples (ND = “no demagnetization”), $B_{\mathrm{c,ND}}$ is independent of the height of the additional sample and can be interpreted as an ideal case, i.e. the upper limit of the attainable field strength using the array. Now focusing on Figure 9 (b), as the height of the additional sample is increased, the field computed with the finite-element model is found to become closer to the maximum field reachable with the array. From all these observations, it can be concluded that the retracting motion of the additional sample induces a re-configuration of the current loops within the central superconductor. While the initial current density distribution is not fully restored, this modification in the current pattern results in an elevation in the magnetic flux density above the centre of the array. The simulations further demonstrate that the efficiency of the proposed method increases when taller additional samples are employed, as taller samples exhibit higher trapped fields.

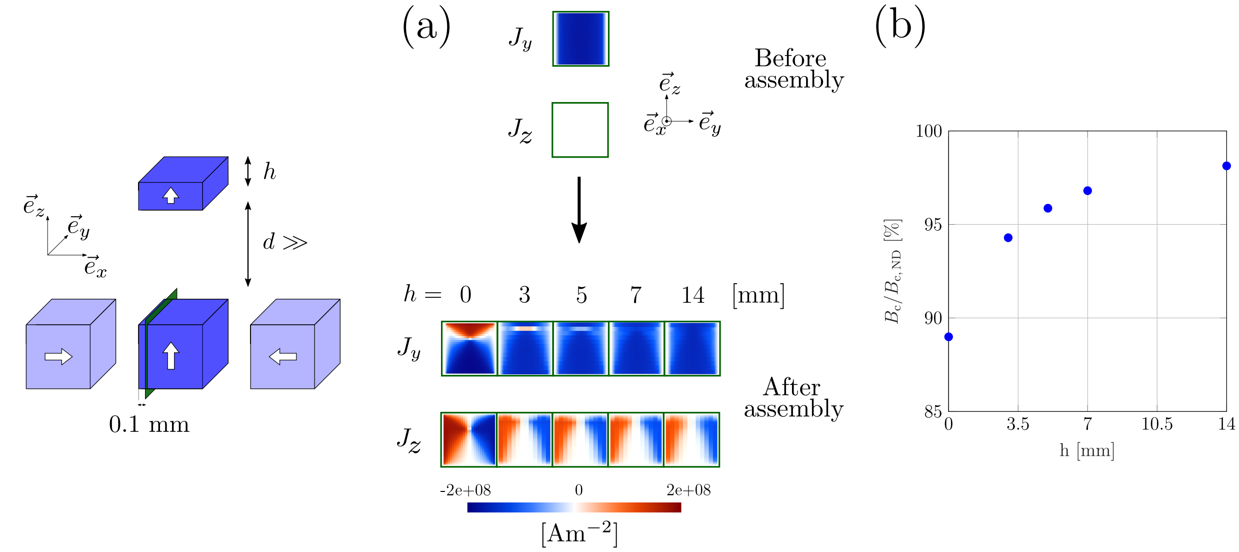

Figure 9. (a) Comparison of the y and z-components of the current density distribution before and after the alternative assembly of a Halbach array made of bulk superconductors computed by the finite element model for several heights of the additional superconductor. The results are presented in a y-z cut plane located at 0.1 mm from the lateral face of the central superconductor. (b) Ratio between the magnetic flux density computed with the finite element model (B_c) and with the analytical model assuming no demagnetization ($B_{c,\,ND}$), 1 mm above the centre of the top surface of the central superconductor and after the alternative assembly procedure for several heights of the additional superconductor. The white arrows represent schematically the main direction of the trapped flux density in each sample. A field-independent critical current density of 2.3×10^8 A m^{-2} is considered in these simulations.

The behaviour of magnetized superconducting stacked-tape samples is also examined through similar simulations. The y-component of the current density computed in two distinct cut planes after the removal of the additional sample as well as the central field computed 1 mm away from the array are presented in Figure 10.

Although the precise final current distribution in the central sample is different from that computed for bulks (as shown in Figure 9 (a)), similar qualitative observations can still be performed when examining the behaviour of stacked tapes. Indeed, it appears in Figure 10 (a) that the use of an additional sample leads to a noticeable modification of the supercurrent pattern within the central stacked tapes. Additionally, it can be observed that as the height of the additional sample is increased, the final distribution of the current becomes qualitatively closer to the initial one. As shown in Figure 10 (b), the field generated above the centre of the structure becomes closer to $B_{c,\mathrm{ND}}$ as the height of the additional sample increases, which suggests that the modification of the supercurrent pattern positively impacts the performance of the array.

The alternative assembly process is then tested experimentally both on a Halbach array made of bulk superconductors and on a Halbach array made of stacked-tape samples. Considering a potential lack of reproducibility arising from the unknown speed during the manual extraction of the additional sample (step c) in Figure 4), each experiment was conducted twice. The relative difference between the central field measured for the two runs of measurements was found experimentally to be smaller than 2 mT, both for the experiment with bulk superconductors and with stacked tapes. Furthermore, we ran the finite element model with two different extraction speeds (1 mm s^{-1} and 10 mm s^{-1}). After allowing a period of 45 minutes of magnetic relaxation after the retract motion, the central field evaluated in the simulation carried out with these two extraction speeds were found to differ by only 3 mT. These observations give confidence that the exact value of the retracting speed of the additional sample has actually little impact on the field generated by the final configuration after magnetic relaxation. The magnetic flux density distributions measured in the first run of each experiment are presented in Figure 11. The experimental data are also compared (i) to the measurements obtained on a classic assembly of the Halbach array and (ii) to the predictions of the analytical model assuming no alteration of the individual magnetization, which can be viewed as the maximum potential of the assembly.

Focusing on the regions above the peripheral samples in Figure 11 (a) and Figure 11 (b), one can notice that the magnetic flux density distribution remains unchanged when the alternative assembly process is used. This result confirms that no significant modification is induced in the peripheral samples during the retract motion of the additional

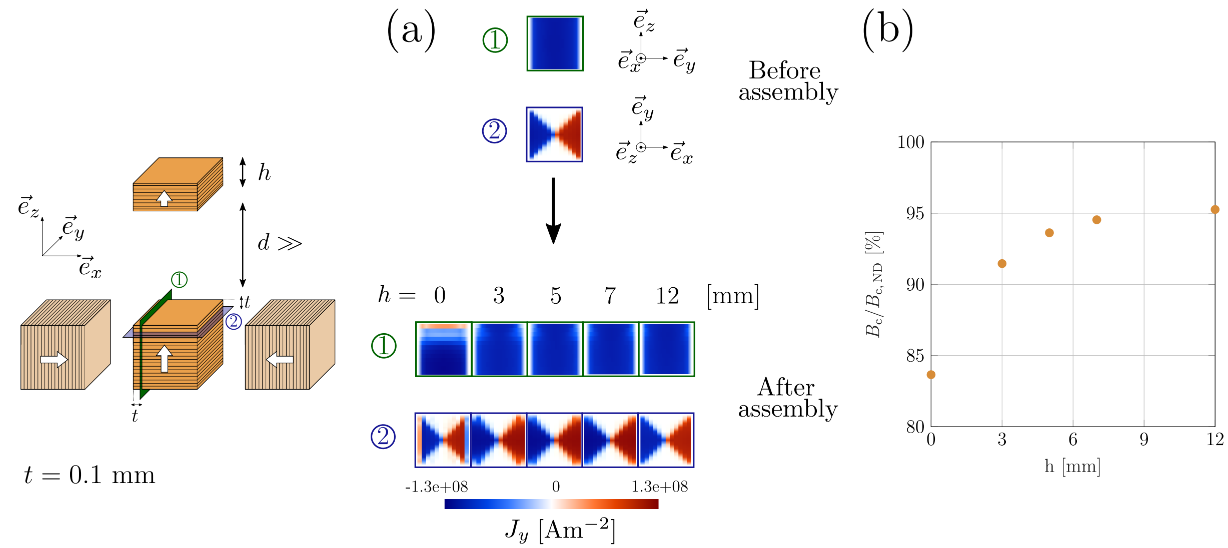

Figure 10. (a) Comparison of the y-component of the current density distribution before and after the alternative assembly of a Halbach array made of superconducting stacked tapes computed by the finite element model for several heights of the additional superconductor. The results are presented in a y-z cut plane located at 0.1 mm from the lateral surface of the central superconductor (Plane ①) and in a x-y cut plane located at 0.1 mm from the top surface of the central superconductor (Plane ②). (b) Ratio between the magnetic flux density computed with the finite element model (B_c) and with the analytical model assuming no demagnetization ($B_{c,\,ND}$), 1 mm above the centre of the top surface of the central superconductor and after the alternative assembly procedure for several heights of the additional superconductor. The white arrows represent schematically the main direction of the trapped flux density in each sample. A field-independent critical current density of 1.7×10^8 A m^{-2} is considered in these simulations.

superconductor. The result differs when considering the experimental magnetic flux density distribution above the central sample, i.e. $|x| < 7$ mm for the bulk superconductors and $|x| < 6$ mm for the stacked tapes. The maximum field generated above the centre of the array is increased when using the alternative assembly process, which gives evidence that a re-magnetization of the central sample occurs. For the bulk superconductors, the maximum field reached with a classic assembly was equal to 471 mT whereas it reaches 495 mT with the alternative assembly, i.e. a 5% increase is measured. For the assembly of stacked tapes, a classic assembly leads to a maximum field of 205 mT against 227 mT for the alternative assembly, i.e. a 11% increase. The alternative assembly method is therefore more efficient for stacked tapes than for bulk superconductors. This fact can be understood when considering the location where the re-organization of the current loops occurs during the approach of the peripheral samples (Figure 7). For bulk superconductors, the supercurrents are altered in a region close to the contact surface between the central and the peripheral superconductors. The behaviour of stacked-tape samples differs significantly as the alteration of the supercurrents occurs in a region close to the top surface of the central superconductor. The additional sample is therefore closer to the regions that needs to be re-magnetized in the latter case and it makes sense to obtain a more efficient re-magnetization.

Finally, Figure 11 shows that the maximum central field predicted by the analytical model ignoring the current redistribution reaches 530 mT and 250 mT for a Halbach array made of bulk superconductors and of stacked tapes respectively, meaning that a further increase of the central field is still possible. This results is fully consistent with the finite element simulations. Using an additional superconductor taller than 5 mm is expected to induce a more efficient re-magnetization. A further increase of the central field of 7% and 9% could potentially be obtained with a Halbach array made of bulk superconductors and of stacked tapes respectively. Note that the force required to extract the additional sample from the configuration increases with the height of the additional sample. This force is evaluated numerically to 15 N with the finite element model for a bulk sample of height 14 mm, such a force strength remains easy to handle. Given that this force scales with the square of the trapped field of individual magnets, it may however become a true challenge when considering superconducting Halbach arrays of larger scale or when exploring the behaviour of superconducting Halbach arrays at lower temperatures.

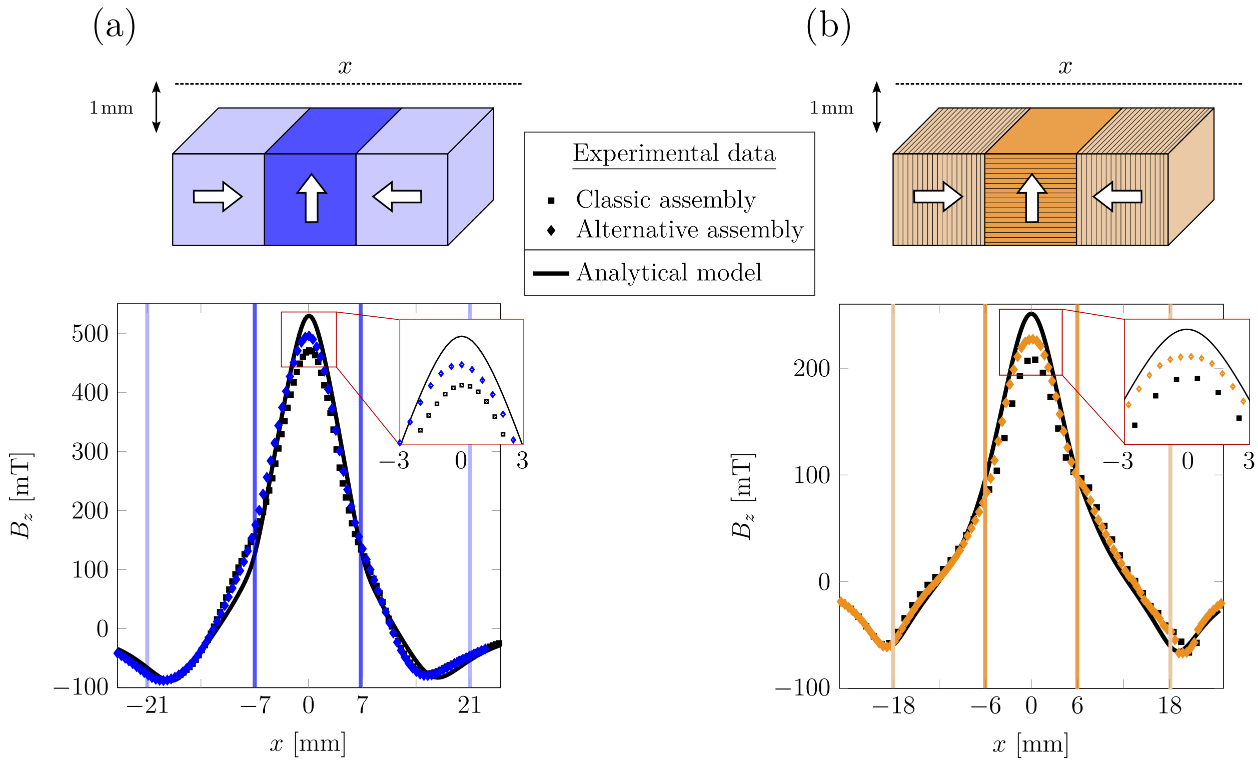

Figure 11. Evolution of the z-component of the magnetic flux density generated 1 mm away from the surface of a Halbach array made up of three superconductors and assembled with the alternative method along the line x. The vertical lines delimitate the borders of the superconducting samples, the white arrows represent schematically the main direction of the trapped flux density in each sample. The experimental data are compared both to the results obtained with a classic assembly process and to an analytical model assuming a simple vector summation of the flux densities generated by each superconductors in the array and no alteration of the individual magnetization. (a) Assembly of 3 bulk YBCO superconductors, (b) Assembly of 3 stacked tapes.

5. Conclusions

Trapped field superconducting magnets arranged in a Halbach array offer the prospect of generating high magnetic fields. During the assembly of the array, however, the increasing field generated by the neighbouring samples induces currents that partially demagnetize the superconductors. In this work we show two ways how this problem can be successfully addressed. We first considered quasi-bulks made of stacked coated conductor tapes. The magnetic flux density generated by 3 permanently magnetized superconducting stacked-tape sampes in a linear Halbach array was investigated experimentally at 77 K. A finite element model based on the mixed h-ϕ-a formulation was developed and successfully reproduced the flux density distribution measured experimentally. The simulations highlight that the field generated by the array is limited by the reorganization of current loops induced in the central stacked-tape sample during the assembly process. Although the occurrence of such loops was observed previously when using bulk superconductors, we showed in this work that the regions of the stacked-tape sample affected by the assembly process differ significantly from their bulk counterparts: the loops generated by the assembly process are confined in the plane of the plates, flow at the periphery of the central stack, mostly on the high-field side of the array. Replacing bulks by stacked tapes was found to have little effect on the demagnetization of the Halbach array.

We then proposed a modified assembly procedure aiming at re-magnetizing the central superconductor of the array after the assembly process. The procedure consists in maintaining two closely spaced magnetized superconductors stationary while approaching trapped field magnets from left and right with their magnetization axes perpendicular to their neighbours. Then, the top central sample is removed from the array. It was shown experimentally that a re-magnetization occurs during the retracting motion of the additional top sample, even if the height of the additional sample is only one third of the height of the main superconductors of the array. Despite not complete, this re-magnetization allowed to increase the maximum field generated with Halbach arrays made of 3 bulk superconductors or 3 stacked tapes by 5% and 11% respectively. Although these enhancements might seem modest as relative quantities, it should be highlighted that the absolute gain can actually be significant, especially when one considers that the present maximum trapped field in a superconductor is 17.6 T [11]. Furthermore, in the context of using a superconducting Halbach array for exerting force on a superparamagnetic particle, the particle experiences a force directly proportional to both its magnetization and the gradient of the magnetic flux density. When the superparamagnetic particle is not saturated, enhancing the field generated by the Halbach array yields a dual positive effect on the applied force: it increases both the generated magnetic flux density gradient and the magnetization of the particle.

Finally, finite element modelling showed that a more efficient re-magnetization is possible with this method by using a taller additional superconductor, which would lead to a higher central field. Provided that the attraction force between the central and the additional superconductor can be handled, the method proposed in this work can be applied with an additional sample presenting higher trapped field. In that latter case, one could expect a Halbach array made of bulk superconductors or stacked tapes respectively to recover almost their full potential.

Acknowledgment

This work was supported by the Fonds de la Recherche Scientifique - FNRS under grant CDR n° J.0218.20 (35325237). Michel Houbart is recipient of a FRS-FNRS Research Fellow grant.

References

[1] K Halbach 1980 *Nucl. Instrum. Methods* **169** 1–10
[2] L C Barnsley, D Carugo, J Owen, and E Stride 2015 *Phys. Med. Biol.* **60** 8303–8327
[3] L C Barnsley, D Carugo, and E Stride 2016 *J. Phys. D: Appl. Phys.* **49** 225501
[4] H Kee, H Lee, and S Park 2020 *J. Magn. Magn. Mater.* **514** 167180
[5] A Omelyanchik, G Lamura, D Peddis, and F Canepa 2021 *J. Magn. Magn. Mater.* **522** 167491
[6] F Fohr, and N Volbers 2018 *AIP Advances* **8** 047701
[7] D Brown, B-M Ma, and Z Chen 2002 *J. Magn. Magn. Mater.* **248** 432–440
[8] M Houbart, J-F Fagnard, J Dular, A R Dennis, D K Namburi, J H Durrell, C Geuzaine, B Vanderheyden, and P Vanderbemden 2022 *Supercond. Sci. Technol.* **35** 064005
[9] S Nariki, H Teshima, and M Morita 2016 *Supercond. Sci. Technol.* **29** 034002
[10] M Tomita, M Murakami 2003 *Letters to Nature* **421** 517–520
[11] J H Durrell, A R Dennis, J Jaroszynski, M D Ainslie, K G B Palmer, Y-H Shi, A M Campbell, J Hull, M Strasik, E E Hellstrom, and D A Cardwell 2014 *Supercond. Sci. Technol.* **27** 082001
[12] A Patel, A Baskys, T Mitchell-Williams, A McCaul, W Coniglio, J Hänisch, M Lao, and B A Glowacki 2018 *Supercond. Sci. Technol.* **31** 09LT01
[13] J R Hull 1999 *IEEE Trans. Appl. Supercond.* **9** ASC98
[14] K Funaki, and K Yamafuji 1982 *Jpn. J. Appl. Phys.* **21** 299–304
[15] A M Campbell, M Baghdadi, A Patel, D Zhou, K Y Huang, Y-H Shi, and T A Coombs 2017 *Supercond. Sci. Technol.* **30** 034005
[16] Z Hong, P Vanderbemden, R Pei, Y Jiang, A M Campbell, and T A Coombs 2008 *IEEE Trans. Appl. Supercond.* **18** 1561–1564
[17] P Vanderbemden, Z Hong, T A Coombs, S Denis, M Ausloos, J Schwartz, I B Rutel, N Hari Babu, D A Cardwell, and A M Campbell 2007 *Phys. Rev. B* **75** 174515
[18] L M Fisher, A V Kalinov, S E Savel'ev, I F Voloshin, V A Yampol'skii, M A R Leblanc, and S Hirscher 1997 *Physica C Supercond.* **278** 169–179
[19] J Srpcic, F Perez, K Y Huang, Y-H Shi, M D Ainslie, A R Dennis, M Filipenko, M Boll, D A Cardwell, and J H Durell 2019 *Supercond. Sci. Technol.* **32** 035010
[20] J Luzuriaga, A Badía-Majós, G Nieva, C López, A Serquis, and G Serrano 2009 *Supercond. Sci. Technol.* **22** 015021
[21] M Kapolka, J Srpcic, D Zhou, M D Ainslie, E Pardo, and A R Dennis 2018 *IEEE Trans. Appl. Supercond.* **28** 6801405
[22] A Patel, K Filar, V I Nizhankovskii, S C Hopkins, and B A Glowacki 2013 *Appl. Phys. Lett.* **102** 102601
[23] T Tamegai, T Hirai, Y Sun, and S Pyon 2016 *Appl. Phys. Lett.* **530** 20–23
[24] M Baghdadi, H S Ruiz, and T A Coombs 2014 *Appl. Phys. Lett.* **104** 232602
[25] M Baghdadi, H S Ruiz, and T A Coombs 2018 *Scientific Reports* **8** 1342
[26] A Baskys, A Patel, and B A Glowacki 2018 *Supercond. Sci. Technol.* **31** 065011
[27] M Kapolka, E Pardo, F Grilli, A Baskys, V Climente-Alarcon, A Dadhich, and B A Glowacki 2020 *Supercond. Sci. Technol.* **33** 044019
[28] D A Cardwell 1998 *Mater. Sci. Eng. B Solid State Mater. Adv. Technol.* **53** 1–10
[29] Y-H Shi, D K Namburi, W Zhao, J H Durrell, A R Dennis, and D A Cardwell 2016 *Supercond. Sci. Technol.* **29** 015010
[30] D K Namburi, Y-H Shi, W Zhai, A R Dennis, J H Durrell, and D A Cardwell 2015 *Cryst. Growth Des.* **15** 1472–1480
[31] D K Namburi, Y Shi, and D A Cardwell 2021 *Supercond. Sci. Technol.* **34** 053002
[32] C P Bean 1962 *Phys. Rev. Lett.* **8** 250–253
[33] A I Podlivaev, I A Rudnev, and N P Shabanova 2014 *Bull. Lebedev Phys. Inst.* **41** 351–354
[34] I A Rudnev, and A I Podlivaev 2016 *IEEE Trans. Appl. Supercond.* **26** 8200104
[35] I Rudnev, D Abin, M Osipov, S Pokrovskiy, Y Ermolaev, N Mineev 2015 *Phys. Procedia* **65** 141–144
[36] J Dular, K Berger, C Geuzaine, and B Vanderheyden 2022 *IEEE Trans. Magn.* **58** 8205204
[37] K Yamazaki 1997 *EEJ* **118** 111–120
[38] H Yamasaki, and Y Mawatari 2000 *Supercond. Sci. Technol.* **13** 202–208
[39] M Houbart, J-F Fagnard, A R Dennis, D K Namburi, Y Shi, J H Durrell, and P Vanderbemden 2020 *Supercond. Sci. Technol.* **33** 064003

Appendix 1: Magnetic flux density on the lateral face of the central superconductor

Given that the current alteration during the assembly process is initiated by the magnetic field produced by the peripheral samples on the side surface of the central superconductor, it is of interest to examine the distribution of the 3 components of this field as they are predicted by the analytical model. In this context, the field generated solely by the left superconductor is computed within a plane that encompasses the contact surface between the left and central superconductors. The results of this calculation are shown in Figure 12.

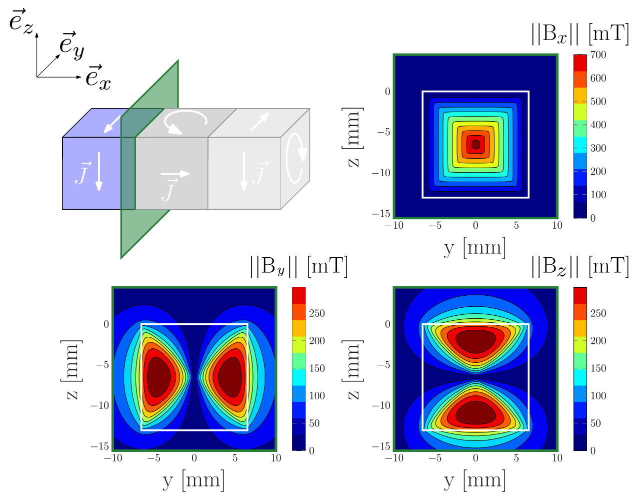

Figure 12. Distribution of the magnetic flux density generated solely by the left superconductor on the lateral face of the central superconductor. The white lines show the location of the border of the central sample.

As can be observed in Figure 12 both the y and z-components of the calculated field are non-zero over the side surface of the central superconductor. More precisely, having a closer look on the distribution of $||B_z||$, it can be highlighted that the area exhibiting high values of B_z according to the analytical model corresponds to the region where a current alteration is predicted by the finite element simulation (refer to Figure 6). This suggests that the z-component of this field is indeed responsible for the current alteration occurring during the assembly process of a superconducting Halbach array made of stacked tapes.